Annu. Rev. Biophys. Biomol. Struct. 2000. 29:497–521
Copyright © 2000 by Annual Reviews. All rights reserved

ELECTROSTATIC MECHANISMS OF DNA DEFORMATION

Loren Dean Williams
School of Chemistry and Biochemistry, Georgia Institute of Technology, Atlanta, Georgia 30332-0400; e-mail: loren.williams@chemistry.gatech.edu

L. James Maher III*
Department of Biochemistry and Molecular Biology, Mayo Foundation, Rochester, Minnesota 55905; e-mail: maher@mayo.edu

Key Words curvature, bending, counterion condensation, groove, collapse

■ **Abstract** The genomes of higher cells consist of double-helical DNA, a densely charged polyelectrolyte of immense length. The intrinsic physical properties of DNA, as well as the properties of its complexes with proteins and ions, are therefore of fundamental interest in understanding the functions of DNA as an informational macromolecule. Because individual DNA molecules often exceed 1 cm in length, it is clear that DNA bending, folding, and interaction with nuclear proteins are necessary for packaging genomes in small volumes and for integrating the nucleotide sequence information that guides genetic readout. This review first focuses on recent experiments exploring how the shape of the densely charged DNA polymer and asymmetries in its surrounding counterion distribution mutually influence one another. Attention is then turned to experiments seeking to discover the degree to which asymmetric phosphate neutralization can lead to DNA bending in protein-DNA complexes. It is argued that electrostatic effects play crucial roles in the intrinsic, sequence-dependent shape of DNA and in DNA shapes induced by protein binding.

CONTENTS

*Corresponding author.

PERSPECTIVES AND OVERVIEW

In this review we discuss electrostatic forces that result in the local deformation of DNA. Four kinds of DNA deformation are considered here: curvature, bending, torsion, and stretching. DNA curvature and DNA bending (10, 25) refer to lateral deviations of the helix axis from a linear trajectory. Curvature refers to nonlinear geometries adopted by double-helical DNA fragments in a specified solvent and ion environment, but in the absence of bound proteins. The extent to which DNA curvature is a property intrinsic to the DNA sequence itself, rather than a response to the solvent and ion environment, is an important issue to be addressed here. DNA bending refers to nonlinear geometries induced in DNA upon binding to proteins. Of specific interest is the role of electrostatic forces in DNA bending and, in particular, how modulation of interphosphate repulsion forces might play a role in DNA bending by proteins. Besides DNA curvature and bending, DNA stretching along the helix axis and torsion about the helix axis are also of interest.

Local curvature and bending deformations of DNA are critical to three aspects of DNA function in cells. First, the extreme length of genomic DNA ($\sim$2 m in the case of diploid human DNA) necessitates remarkable but reversible compaction for storage. The detailed basis of DNA compaction in nuclei and viruses is not fully understood but involves DNA wrapping or spooling on protein scaffolds or condensation with other oligocationic substances (5). Second, it appears likely that DNA sequence information is detected to some extent by "indirect readout," that is, sequence-specific DNA shapes that modulate interaction with DNA-binding proteins. Deformed (or deformable) DNA sequences may provide cues allowing the proper positioning of machinery that detects punctuation signals in genomes (62). Third, DNA deformation is required for the integration of DNA sequence information encoded at remote sites. Thus, DNA sequences specifying binding

sites for regulatory proteins are frequently separated by relatively long distances, yet proteins bound to these sites often sense one another "at a distance," displaying cooperativity in function. Integration of remote sequence information is typically understood in terms of DNA bending and looping to bring remote binding sites into proximity. DNA deformation is particularly important because naked DNA behaves as a locally stiff polymer in aqueous solution.

MEASURES OF DNA STIFFNESS

Persistence Length

DNA stiffness can be described in terms of several measurable parameters (56). One measure of DNA stiffness is longitudinal persistence length P [$\sim$150 bp at 25°C, 0.2 M ionic strength (8, 35)], formally defined as the average projection of the molecular end-to-end distance vector on its initial path vector, in the limit of infinite chain length (8, 24). Persistence length is thus a measure of the resistance of a polymer to lateral bending. Various other interpretations of persistence length are also helpful. For example, as DNA length decreases below the persistence length, the molecular behavior approaches that of a rigid rod with elastic resilience (24). This rigid-rod approximation becomes particularly applicable to DNA fragments of $\sim P/2$ ($\sim$75 bp). Another useful interpretation of persistence length is the distance over which the root-mean-square (rms) bend angle in any particular direction is 1 rad ($\sim$60°). Thus, under the conditions specified above, the helix axis of an average DNA molecule changes direction by $\sim$60° over every 150-bp segment.

It should be noted that, although DNA is locally rather stiff, very long DNA molecules are globally flexible such that the average end-to-end molecular distance approximates $(PL)^{0.5}$, where L is the molecular contour length. Thus, the approximate end-to-end distance for a continuous DNA double helix encoding the human genome ($\sim 3 \times 10^9$ bp) would not be 1 m (its contour length), but rather 230 μm owing to global DNA flexibility. However, because animal cells have typical diameters of 10–30 μm and typical nuclear diameters of 5–7 μm, it is evident that random coiling provides insufficient compaction for DNA packaging. DNA spooling onto histones and subsequent higher-order interactions are therefore required.

Torsional Rigidity

DNA also displays local stiffness in torsion. This property can be expressed in terms of a "torsional" persistence length, that is, the length over which DNA tends to resist twisting about the helix axis. By analogy to longitudinal persistence length, the DNA length required to give an rms twist deviation of 1 rad ($\sim$60°) from the initial reference frame can be defined as the torsional persistence length T, which has a calculated value of $\sim$180 bp, a value similar to the longitudinal

persistence length *P* (J Kahn, personal communication). Remarkably, the DNA distance required for two sites to become insensitive to torsional phasing (i.e. to obtain an rms torsional deviation of 180°) is ∼2000 bp. Thus, over shorter distances, strong face-of-the-helix (phasing) effects can be reasonably expected for bound proteins.

The combination of lateral and torsional DNA stiffness has profound implications for three-dimensional nucleoprotein structures involving DNA. Because of this inherent stiffness, the biologically relevant bending and folding of DNA into compact nucleoprotein structures such as nucleosomes (53), recombination complexes (21), and transcription complexes (19, 35, 69) require energy if DNA is to be deformed more extremely than indicated by the persistence parameters described above. This energy is provided by favorable protein-DNA interactions involving van der Waals contacts, burial of hydrophobic surfaces, formation of hydrogen bonds, and ion pairings that release counterions. Many or all of these forces presumably play roles in the alteration of DNA shape by proteins.

A second key implication appears in calculations of the effective relative concentrations of DNA sites (or proteins bound to them) by virtue of their occurrence on the same DNA molecule. Such effective concentrations are equivalent to *j* factors (3, 74, 81) and reflect the frequency of intramolecular collisions between specified DNA sites. Model calculations accounting for DNA stiffness show that two sites on DNA collide most frequently when they are separated by ∼500 bp, creating an effective concentration in excess of 1×10^{-7} M (74, 81). Under appropriate conditions, two proteins bound to such sites are held at higher local concentration via the DNA tether than when the proteins are free in solution. More closely spaced sites collide less frequently owing to the stiffness of the intervening DNA; at 150-bp separation, the effective concentration of one DNA site in the presence of another is only $\sim 2 \times 10^{-9}$ M (∼50-fold lower than maximum). Sites separated by DNA lengths >∼500 bp also experience lower effective concentrations owing to dilution as each site samples a greater volume of space: at ∼3000 bp of separation, the effective concentration of two tethered sites is reduced to $\sim 2 \times 10^{-8}$ M (∼fivefold lower than maximum). These considerations emphasize the importance of local DNA curvature and/or bending in altering the degree to which proteins sense one another when bound to a common DNA molecule.

When two DNA sites are defined on specific faces of the double helix, effective concentrations also oscillate in a sinusoidal manner as a function of separation distance, reflecting the helical periodicity of the double helix. Optimal vs nonoptimal helical phasing may alter the effective concentration of two sites by five- to tenfold over separation distances of 60–200 bp because of torsional rigidity (74).

Young's Modulus

Besides resisting longitudinal and torsional deformation, DNA resists stretching beyond the contour length associated with its canonical B form. Resistance to such stretching is characterized by an elastic stretch modulus, *S*, which, when divided

by the cross-sectional area of the polymer, gives the familiar Young's modulus, E. Recent innovative single-molecule stretching experiments with phage λ DNA have provided estimates for S (2). Interestingly, the measured longitudinal persistence length P was observed to be roughly constant between 10 mM and 600 mM ionic strength, whereas the elastic stretch modulus S increased dramatically: overstretching DNA was easier at low ionic strength. Interpreting the observed relationship between P and S will require additional studies.

CONTRIBUTIONS OF INTERPHOSPHATE REPULSIONS TO DNA STIFFNESS

What accounts for the stiffness of DNA? Surprisingly, the answer to this fundamental question remains unresolved. Various possibilities can be considered. In one view, the tendency to maximize base stacking is the dominant force resisting DNA deformations such as lateral bending, torsion, and stretching. On the other hand, mutual interphosphate repulsions (and their interactions with the local base-pair dipoles) might cause DNA rigidity by resisting deformed conformations, which crowd phosphate groups. In yet another view, DNA stiffness reflects an equilibrium between forces that tend to compress the DNA (such as base-pair stacking) and interphosphate repulsions (which tend to stretch it). Estimating the relative contributions of base stacking and electrostatic repulsions to DNA stiffness and deformation remains an important and active research area. This review considers the evidence that local electrostatic effects contribute substantially to intrinsic DNA curvature and to DNA bending induced by bound ligands and proteins.

Counterion Condensation Theory

Critical to a discussion of electrostatic effects in DNA is an appreciation for the counterion condensation phenomenon associated with densely charged polyelectrolytes. Many sophisticated analyses and simulations have been applied to understanding the distribution of counterions around DNA (27, 60, 61). The elegant theory of Manning (55) remains a useful framework for interpreting the thermodynamic behavior of DNA in solutions of ions. Manning proposed that the high negative charge density of DNA induces a concentrated cloud of mobile and hydrated counterions within ∼7 Å of the DNA surface. For monovalent cations, the ionic concentration in this cloud approaches 1 M and is relatively independent of the bulk cation concentration. This "condensed" layer of counterions is sufficient to neutralize ∼76% of the DNA charge, thereby reducing the charge of each phosphate (in a thermodynamic sense) to $-0.24\,e$. This model indicates that divalent and trivalent counterions reduce residual phosphate charge to $-0.12\,e$ and $-0.08\,e$, respectively (55). This analysis has two particularly important implications. First, the electrostatic contribution to DNA stiffness is reduced by phosphate screening owing to counterion condensation. Second, the binding of cationic ligands to

DNA is an ion-exchange reaction in which condensed counterions are released into bulk solvent, providing an important favorable entropic source of binding energy (70, 71).

DNA Persistence Length and Ionic Strength

Does the predicted residual phosphate charge of −0.24 (monovalent salt) contribute to polymer stiffness under physiological ionic conditions? Under such conditions, the Debye screening length, κ^{-1}, is ∼10 Å (∼3 bp), suggesting that, if interphosphate repulsions contribute substantially to stiffness, they must do so through local interactions (8, 57). A seemingly direct approach to estimating the electrostatic contribution to DNA stiffness has been to measure the longitudinal persistence length of DNA as a function of monovalent cation concentration (reviewed in 24). A particularly interesting recent example is the measurement of single-molecule DNA elasticity (related to persistence length) in the presence of different concentrations of counterions of different valences (2). For monovalent salt, these authors found:

$$P = P_0 + 0.324I^{-1} \qquad 1.$$

where P_0 (500 Å) is the nonelectrostatic contribution to longitudinal persistence length in Å and I is ionic strength in molar units. Thus, the stiffness of DNA as measured by persistence length in dilute solution appears to decrease dramatically as monovalent cations are added, reaching an invariant value of ∼500 Å under physiological conditions.

The independence of longitudinal persistence length from cation concentration in the physiological range (as cited above) remains a subject of some dispute (24, 26, 55). If P achieves some constant "saturated" value above an ionic strength of 50 mM, it is tempting to conclude that interphosphate repulsions are completely screened under physiological conditions ($I \geq 140$ mM) and therefore make no contribution to DNA stiffness over this range of ion concentrations. In contrast, Manning's theory predicts that residual phosphate charges should make a constant local contribution to stiffness (55). That an electrostatic contribution to P persists above 100 mM ionic strength is suggested by the fact that multivalent cations such as Mg^{2+} [predicted to reduce residual phosphate charge from −0.24 to −0.12 (55)] drastically reduce persistence length (2). Persistence lengths below 300 Å were estimated for DNA in the presence of certain multivalent cations (2). The mechanism for this reduction in P is unknown. Bloomfield and coworkers suggest that transient and random multivalent cation binding and bending of DNA may be occurring (2, 76). An alternative interpretation is that counterions of higher valance lower residual phosphate charge in accord with counterion condensation theory (55), reducing interphosphate repulsions and decreasing DNA stiffness.

It is important, however, that P is not the only measure of DNA flexibility. For example, interphosphate repulsions may also contribute to the elastic stretch

modulus of DNA, *S* (2). Thus, deducing the contribution of interphosphate repulsions to DNA stiffness from the dependence of *P* on *I* remains problematical.

Results of other recent experiments suggest that DNA-like molecules remain stiff even when their formal axial charge density is reduced by a factor of two. Hagerman & Hagerman allowed methylated monomeric adenosine nucleosides to spontaneously assemble into metastable "meroduplexes" on a complementary single-stranded poly(deoxythymidylate) (23). Using transient electric birefringence (TEB) analysis, these authors fit relaxation data to persistence length models and concluded that the hemi-charged meroduplex had a persistence length approaching that of duplex DNA. This intriguing result suggests that base stacking interactions predominate over interphosphate repulsions in determining *P*, although a role for local phosphate neutralization in modifying helix trajectory is not ruled out.

Interphosphate Repulsions and Persistence Length

Is it reasonable to expect that interphosphate repulsions should contribute strongly to persistence length? When DNA is laterally bent, phosphates on the inner face of the bend experience crowding. However, such a deformation simultaneously increases interphosphate distances on the opposite face of the site of bending, such that the costs associated with phosphate crowding on one face and the favorable energy of interphosphate stretching on the opposite face might tend to cancel. Compensation between phosphate crowding and stretching is observed when interphosphate distances are examined in bent DNA from the nucleosome crystal structure (53). Thus, the net electrostatic bending energy may be small in such cases, not because phosphate repulsions are fully screened but because they tend to cancel on opposite sides of the helix.

Manning Theory of Interphosphate Stretching Forces

Manning approached the problem of the electrostatic contribution to DNA rigidity by placing the focus on interphosphate stretching forces within the double helix (57). This theory proposes that the stable double-helix structure of DNA represents an equilibrium between stretching forces (caused by interphosphate repulsions) and compressive forces (caused by attractive interactions between nucleotides such as, but not necessarily limited to, stacking forces between base pairs). Manning estimated the stretching force as the partial derivative of DNA free energy as a function of length, thereby relating this force to the linear charge density and the Debye charge screening parameter. The theory requires no assumptions about the salt dependence of *P*, and a conventional value for *P* was used in calculations. The result of this analysis suggested that significant local interphosphate stretching forces balance compressive forces within DNA and that these stretching forces can drive DNA deformation when phosphate charges are locally neutralized. In particular, asymmetric phosphate neutralization (as might be induced by nonhomogeneous counterion density or the presence of a cationic protein bound

to one DNA face) was predicted to result in significant asymmetric interphosphate stretching forces and DNA deformation. In the following discussion, we interpret electrostatic contributions to both DNA intrinsic curvature and induced bending in the context of this theory.

ELECTROSTATICS AND INTRINSIC DNA CURVATURE

Sequence-Dependent Shapes and Traditional Interpretations

Traditional analysis of high-resolution DNA structures, originating with "Calladine's Rules" (7), focuses on direct base-base interactions. Estimates of the relative importance of various types of base-base interactions and other conformational restraints have evolved over time, yet the essential heterocycle-centric, nonelectrostatic nature of the traditional paradigm has not. It has been proposed that direct base-base interactions vary with sequence and modulate relative orientations of bases and base pairs, thereby causing intrinsic curvature (11, 12). In these models, DNA can also be bent by external "leverage forces" exerted by proteins. These traditional models discount contributions from Manning's electrostatic stretching forces. Along with other deficiencies, traditional models deny the central role of electrostatics that is demanded by the effects of salt on intrinsic curvature of A-tracts (13, 48, 80) and G-tracts (6, 14, 89). By contrast, in electrostatic models DNA bends spontaneously when electrostatic forces are asymmetric. For example, an explicit treatment of dynamical characteristics of divalent cations described by Rouzina & Bloomfield (76) suggests that DNA curvature arises from short-range electrostatic interactions between phosphate groups and mobile divalent cations. An analogous conclusion was obtained by Stigter (86).

Role of Ions in Determining Intrinsic DNA Shape: Hybrid Solvent Model

History We believe that an artifactual and unphysical charge imbalance in three-dimensional structures of DNA has contributed to the underestimation of the importance of electrostatics. The seminal "Dickerson dodecamer" [CGCGAATTCGCG, 2.5-Å resolution, Nucleic Acid Database (NDB) entry DBL001 (100)], which spawned the heterocycle-centric paradigm, contains DNA and site-bound water molecules, but no cationic counterions. Observation of monovalent cations such as sodium is particularly problematic. Even at very high resolution, Williams and coworkers directly observed only a magnesium ion and a partial spermine molecule among >150 water molecules [NDB entry BDL084, 1.4-Å resolution (82, 83)] associated with the Dickerson dodecamer. This charge imbalance is a general phenomenon that extends to essentially all nucleic acid structures. The 76 phosphates of the highest-resolution tRNA structure [NDB entry trna10, 2.5-Å resolution (32, 33)] are predominantly unneutralized. The tRNA structure contains only four magnesium ions and no monovalent cations. The apparent charge

imbalance persists in complexes of nucleic acids with cationic proteins. In the nucleosome core particle [NDB entry pd0001, 2.8-Å resolution (53)], 290 phosphate groups are compensated for by only 162 cationic amino acids and 6 divalent cations. This count underestimates the imbalance by ignoring anionic amino acid residues.

Williams and coworkers have proposed a hybrid-solvent model (82, 83) that is consistent with the near invisibility of monovalent cations to X-ray diffraction. In this model, cations distribute asymmetrically around DNA, and solvent sites that were previously characterized as pure water are hybrids, which are partially occupied by monovalent cations (Figure 1; see color insert). The greater occupancies of water over monovalent cations in hybrid solvent sites present difficult analytical challenges during X-ray structure determination. However, these challenges are now being at least partially overcome with high-resolution data, ion substitution, and other techniques (82, 83, 96).

In purely polyelectrolyte solution models, cations around DNA are mobile and are distributed with radial dependence (70, 71). Several lines of evidence suggest that a modest modification of these powerful models may be in order. The mobile cation atmosphere, whether monovalent or divalent, appears to be perturbed by DNA functional groups and is sequence dependent. Crystallographic observations of monovalent cation-water hybrids within the minor groove of A-tracts (82, 83, 96) suggest selective partitioning into that region. In addition, fully hydrated magnesium ions have been shown to avoid DNA amino groups in X-ray structures (83), consistent with nuclear magnetic resonance (NMR) evidence for perturbations of divalent cations from purely radial distributions in solution (29). The influence of DNA functional groups on cation distribution appears to cause a superimposition of peaks and troughs on purely polyelectrolyte radial cation distributions.

Additional Evidence of Influence of DNA Functional Groups on Cation Distributions The first observation of a cation within the minor groove of an AT-tract was made in 1973 by Rosenberg et al, who used single-crystal diffraction to identify a sodium ion near the floor of an abbreviated minor groove of a dinucleotide duplex (75). The relevance of that structure was discounted during initial interpretations of the Dickerson dodecamer. Those interpretations described a purely aqueous "spine of hydration" in the AT-tract minor groove (46). However, additional support for monovalent cations within the minor groove of AT-tracts was provided by Bartenev and coworkers, using fiber diffraction (1). The fiber and single-crystal data are supported by results obtained with DNA in solution. Hud et al demonstrated that ammonium binds preferentially in AT-tract minor grooves (31). These authors have established isotopically labeled ammonium as an excellent NMR probe for monovalent alkali ions in both B-DNA and quadruplex DNA (30). The combined experimental results are consistent with a series of nanosecond-level molecular dynamics simulations, by Young & Beveridge (101) and Young et al (102), of DNA fragments under various salt conditions. In

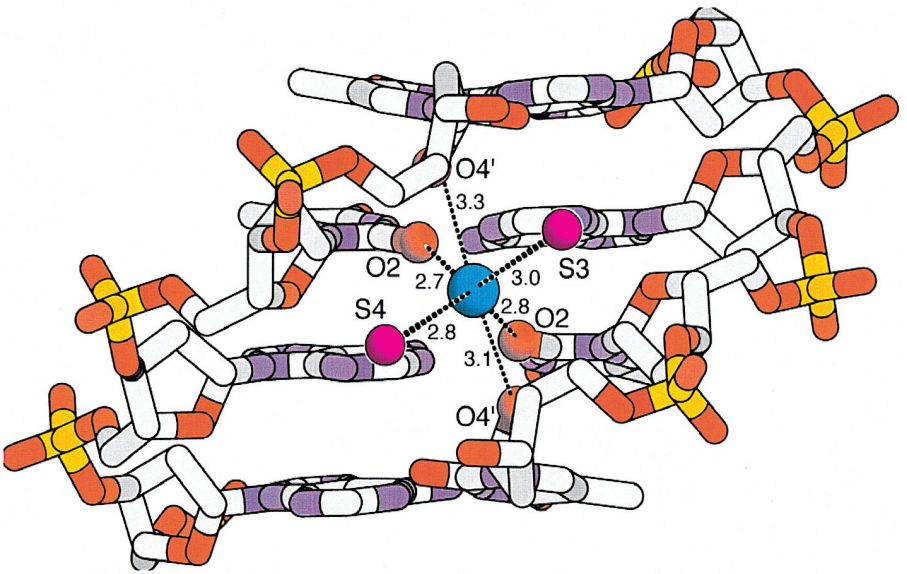

Figure 1 A view into the minor groove of [dCGCGAATTCGCG]2 showing the coordination geometry at the 5′ ApT 3′ step. The atoms are colored by type, with O, *orange*; P, *yellow*; N, *violet*; and C, *white*. The ligands of the water-cation hybrid, represented as spheres, are two O4′ atoms, two thymine carbonyl oxygen atoms (O2), and two occupants of the secondary hydration layer (S, *magenta*). The sphere representing the water-cation hybrid (*blue*) is large than the other six spheres. Distances indicated are in Å.

those molecular dynamics simulations, monovalent cations bind preferentially in AT-tract minor grooves. Thus, a view emerges in which DNA curvature is not seen as intrinsic to the double helix in isolation but is the response of DNA to sequence-dependent asymmetries in the distribution of counterions.

ELECTROSTATICS AND DNA BENDING BY PROTEINS

Classes of DNA-Bending Proteins

High-resolution structural data reveal at least two motifs for DNA bending by proteins (Figure 2; see color insert). These two motifs suggest different underlying mechanisms. One class of DNA-bending proteins (class 1) contacts bent DNA on its convex surface, inducing the helical axis to curve away from the bound protein (54). Such proteins include the TATA-binding protein TBP (40, 42), high-mobility-group proteins such as the human male sex-determining factor SRY, and the lymphoid enhancer-binding protein 1 (68, 98), as well as other proteins that are often classified as "architectural" binding proteins (9, 98, 99). DNA bending by proteins in this group appears to involve intercalation of hydrophobic amino acids between base pairs in the minor groove of DNA, causing DNA unwinding to enlarge the minor groove and alter the helix axis (98, 99). It has been suggested that the relatively low dielectric character of the intercalated protein enhances specific interphosphate repulsions, contributing to DNA deformation (16).

A second class of DNA-bending proteins (which we have termed class 2) includes the *Escherichia coli* catabolite activator protein CAP (79), the histone octamer, responsible for the remarkable wrapping of ~150 bp of DNA by ~720° in nucleosomes (53), and the *E. coli* integration host factor IHF (72). Many other class-2 DNA-bending proteins have been described (43, 51, 67). Class-2 proteins contact bent DNA on its concave surface, curving the helical axis toward the bound protein. The engaged surfaces of class-2 proteins typically present cationic amino acids to the DNA, suggesting that electrostatic interactions are important for DNA binding by these proteins. How such electrostatic interactions contribute to DNA bending is an interesting question.

DNA Bending and Looping Energetics

Proteins that bend DNA do so because their binding free energy is sufficient to pay the energetic cost of deforming the relatively stiff double helix. Simplification of an expression for the free energy of DNA bending (35) leads to Equation 2:

$$\Delta G_{\text{bend}} = 0.0135 \frac{(\Delta\Theta_{\text{deg}})^2}{L_{\text{bp}}} (\text{kcal/mol}), \qquad 2.$$

where the DNA-bending free energy at room temperature is expressed in kilocalories per mole, assuming a DNA persistence length of 150 bp. Equation 2 applies to the bending DNA by $\Delta\Theta$ degrees over a contour length of L_{bp}. When applied to

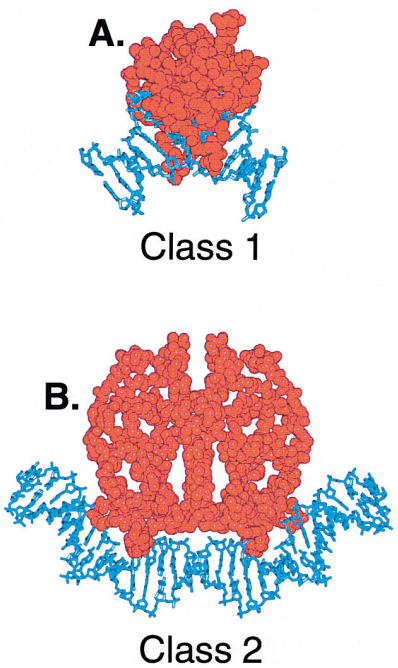

Figure 2 Classes of DNA-bending proteins. A. Class-1 bending proteins (TBP, *red*) bind the DNA minor groove, unwind DNA, and induce bending away from the protein-DNA interface by intercalation of hydrophobic-amino-acid side chains between base pairs. B. Class-2 bending proteins (CAP, *red*) form complexes in which DNA bends toward the protein-DNA interface.

DNA bending on the scale of the nucleosome, this equation suggests that bending ~75 bp of DNA into a circle requires >22 kcal/mol of energy. The equilibrium constant for spontaneous curvature of a 75-bp DNA segment into this shape is 3×10^{-18}, demonstrating that favorable protein-DNA interactions are essential to drive DNA bending in such a structure.

What are the probable sources of this bending energy, and what is the relative importance of each source? Unfavorable energetic contributions to DNA bending by histone binding include both electrostatic and nonelectrostatic costs of bending the DNA. Favorable contributions to DNA bending by proteins presumably arise from the formation of new hydrogen bonds, van der Waals contacts, release of water from interacting nonpolar surfaces, and electrostatic interactions including Coulombic attraction between cationic protein side chains and DNA phosphates and release of condensed counterions upon protein binding (70, 71).

Just as the case has been made for a dominant role of local electrostatics in determining DNA shape in the presence of small ions, a similar argument can be considered for DNA bending by proteins. Thus, the presence of a bound protein must alter the electrical potential experienced by the DNA and its associated ions. How the DNA relaxes in response to these changes is of interest.

The mechanism by which DNA collapses around a cationic protein can be conceptualized in several ways. For example, class-2 proteins often engage the double helix via a convex surface containing multiple cationic side chains. Coulombic attraction between these side chains and the negatively charged DNA surface provides an intuitive driving force favoring the bending of DNA to maximize favorable electrostatic interactions. Perhaps an equally valid view considers maximization of the favorable entropy of counterion release when DNA bends to enhance surface contact with the protein.

Rich-Mirzabekov-Manning Predictions

A related view of the DNA-bending process was originally suggested by Mirzabekov & Rich (59) and was subsequently addressed mathematically by Manning and coworkers as described above (57). This hypothesis grew from the observation that $tRNA^{phe}$ appears to collapse around a groove-bound oligovalent cation (73). It was reasoned that the approach of a cationic protein side chain to a DNA phosphate is equivalent to canceling the residual negative charge of that phosphate: the fixed charges within the DNA experience pairwise electrostatic attractions (to the cation) and repulsions (from the phosphate). These attractive and repulsive forces cancel as the cation and phosphate are juxtaposed. Asymmetric neutralization of partial DNA phosphate charges by the cationic surface of a class-2 protein is thus predicted to alter the balance of electrostatic forces within the DNA double helix. Using an engineering analogy, Manning and coworkers calculated that modest asymmetric phosphate neutralization would create net local compressive forces within the double helix sufficient to account for the degree of DNA bending observed in the nucleosome (57).

Experiments to Isolate and Detect Collapse Forces

In their theory of DNA bending by asymmetric phosphate neutralization, Manning and coworkers introduced the concept of a phantom protein (57). This concept refers to a model in which the electrostatic consequences of protein binding to DNA are isolated from all other forces. Motivated by this idea, Strauss & Maher simulated the electrostatic consequences of protein binding by chemical synthesis of DNA duplexes in which the phosphate charge distribution was altered by partial substitution with neutral phosphate analogs (87). DNA shape was then indirectly monitored by electrophoresis experiments. Figure 3 depicts the molecular design of the original experiment (87) in which six phosphates flanking the DNA minor groove (oxygens are shown in white) were neutralized by methylphosphonate substitution in different phasings compared with an intrinsically curved

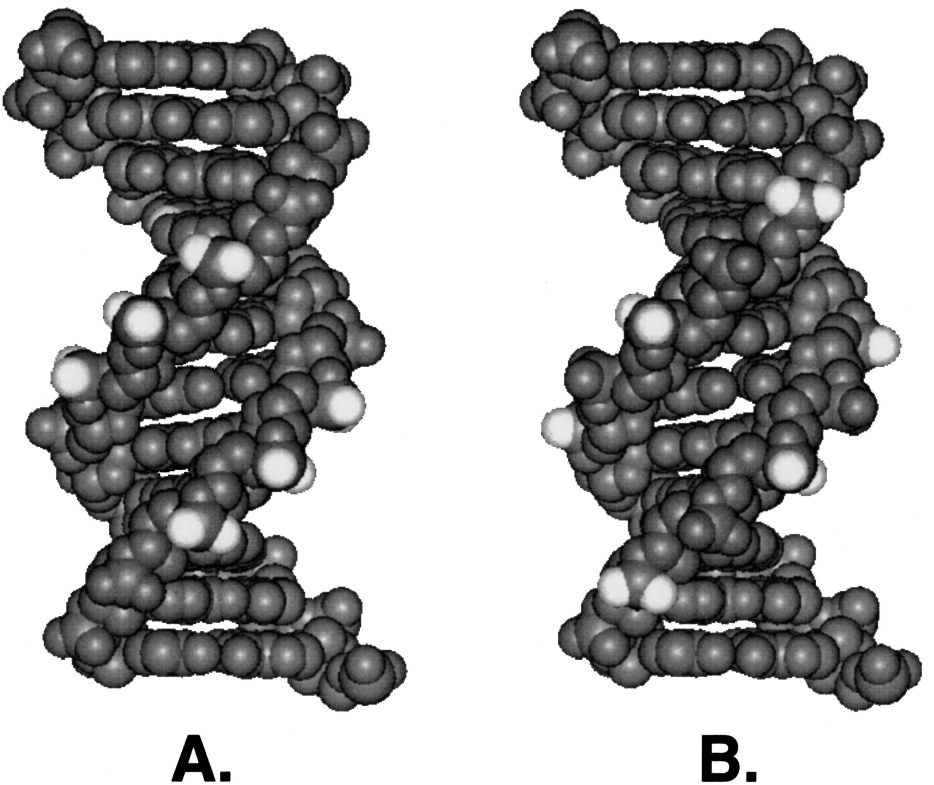

Figure 3 Phantom protein design. Synthetic DNA duplexes in which selected phosphates are chemically neutralized by substitution of methylphosphonate analogs. *White spheres* indicate positions of methyl groups in racemic mixtures. *A.* Neutralization of consecutive phosphates across the minor groove. *B.* Neutralization of alternating phosphates across the minor groove.

A_6 tract. Duplexes were ligated end-to-end for electrophoretic assays (10). In support of the model in question, these studies have consistently shown that asymmetric phosphate neutralization causes DNA bending in the predicted direction. DNA bending would not be anticipated in these model systems if the mechanism of class-2 proteins involved only maximization of favorable charge-charge interactions between protein and DNA, because no proteins were present in these experiments.

The initial study of DNA bending by asymmetric substitution of methylphosphonate linkages showed that $\sim 20^\circ$ of bending results when three phosphates on each side of one minor groove are neutralized (87). Realistic patterns of phosphate neutralization in protein-DNA complexes may be more diffuse. It was of interest to determine whether such a diffuse patch of neutralization (i.e. alternating neutralized and anionic phosphates) changes the extent of DNA bending compared with bending by consecutive neutralized phosphates. Synthetic duplexes were therefore created to measure DNA bending by alternating neutral methylphosphonate residues (racemic) and anionic phosphate diesters in a patch on one face of duplex DNA (91). Overall, the electrophoretic phasing data confirmed that the patch of alternating racemic methylphosphonate/diester linkages induced bending toward the minor groove, enhancing the A_6 tract bend. Calculations indicated that the magnitude of the bend angle caused by the patch of alternating racemic methylphosphonate/diester linkages was $\sim 13^\circ$ toward the minor groove. This result was in qualitative agreement with the previous observation that a patch of consecutive racemic methylphosphonate linkages induces an $\sim 20^\circ$ DNA bend toward the minor groove (87).

Analyses of DNA bending by methylphosphonate substitution assumed that electrostatic effects, rather than steric perturbations, are the major consequences of DNA modification. Methylphosphonate incorporation into synthetic oligomers converts the achiral diester to mixtures of diastereomers at each asymmetric phosphorus atom. Using the bending data obtained for alternating racemic methylphosphonate/diester linkages, Strauss and coworkers created synthetic DNA duplexes with purified dimer synthons of defined methylphosphonate stereochemistry to test effects on DNA bending. Results with chirally pure oligomers were qualitatively similar to those observed for duplexes with a patch of alternating racemic methylphosphonate/diester linkages groove (87). The patch of alternating R_P methylphosphonate/diester linkages induced $\sim 9^\circ$ of DNA bending. It was notable that DNA bending by pure R_P methylphosphonate isomers was somewhat reduced compared with racemic mixtures of methylphosphonates ($\sim 9^\circ$ versus $\sim 13^\circ$), although the predominant electrostatic effect was still clearly detectable. One interpretation of these data is that both R_P and S_P methylphosphonate isomers contribute to DNA bending by electrostatic mechanisms. In addition, however, S_P isomers may perturb DNA structure in a subtle manner through nonelectrostatic effects such as differential solvation or unfavorable steric contacts in the major groove. The latter class of contacts may then induce structural changes that tend to exaggerate modestly the electrostatic contribution to DNA bending.

Independent evidence that asymmetric phosphate neutralization can provide a theoretical force for DNA bending comes from a series of recent computer simulations. Sanghani and coworkers (78) used the JUMNA nucleic-acid-modeling program to predict DNA bending on asymmetric charge neutralization in simulated poly(dA)·poly(dT), poly(dG)·(dC), and poly(dTA)·poly(dTA) polymers. Base sequence had a minor effect on the observed bending. The degree of bending increased when neutralization was increased from 4 phosphates to 6 phosphates, remaining unchanged when 8 phosphates were neutralized and decreasing when the neutralization was increased to 10 phosphates. Earlier simulations by Swarnalatha & Yathindra showed no DNA bending when structures of short, uniformly neutralized DNA duplexes were simulated (94). This result would be expected, because it is the asymmetry in phosphate neutralization that is predicted to cause bending.

Gurlie and coworkers extended application of the JUMNA modeling program to the recognition sequence for the *E. coli* CAP protein (22). These authors made several interesting observations. (*a*) The CAP recognition sequence would possess intrinsic curvature (38°) that is amplified to 51° by CAP protein binding. (*b*) A subset of three neutralized phosphates was sufficient to generate much of this protein-induced bend. (*c*) There was an unexpected dependence of bending on sequence context; when the neutralized phosphates were shifted along the helix, induced bending was reduced. (*d*) Analysis of normal modes in the simulations suggested that phosphate neutralization reduced oligomer flexibility.

A subsequent simulation of asymmetric phosphate neutralization was used to study effects on DNA bending of neutralization pattern and explicit methylphosphonate stereochemistry in the context of a 12-bp alternating poly[d(CG)·d(CG)] duplex (47). Energy optimization of these B-like dodecamers with six phosphate neutralizations confirmed the induction of bending toward the neutralized DNA face. Detailed studies of the effects of stereochemistry showed that homogeneous R_P or S_P methylphosphonate substitutions gave somewhat different bend directions and magnitudes than those predicted by a "pure" mathematical neutralization of phosphate oxygens, a result consistent with previous studies (91). Interestingly, incorporation of racemic mixtures of R_P and S_P methylphosphonate stereoisomers resulted in DNA bending comparable with that predicted for "pure" phosphate neutralization. This important result supports the validity of experimental data obtained in such racemic systems (87, 92). In these simulations, however, the magnitude of DNA bending ($\sim$10°) was somewhat smaller than had been estimated from electrophoretic experiments ($\sim$20°).

The significance of DNA bending observed in computer simulations of asymmetric phosphate neutralization is largely dependent on the quality of the force fields used. To date, such simulations have not included explicit solvent or counterions. On one hand, this limitation exemplifies the rudimentary nature of these studies. On the other hand, DNA bending observed in these studies demonstrates that electrostatic collapse is predicted without invoking the redistribution of specific solvent and/or counterion molecules.

Strauss and coworkers reasoned that covalent tethering of ammonium ions to one face of the DNA double helix might provide an alternative method to simulate asymmetric phosphate neutralization caused by the cationic amino acids of a bound protein. Primary amines (positively charged at neutral pH) were attached via propyl (88) or hexyl (89) tethers to position 5 of pyrimidine residues in synthetic oligonucleotides. This design simulated the approach of six lysine residues near the phosphate backbone on one face of the double helix. As controls, neutral acetylated derivatives of these tethered amines were also analyzed. Appended cations were phased in relation to intrinsic curves caused by A_5-tracts in electrophoretic phasing assays. Quantitative data analysis demonstrated that the $5'$-A_3GT_3 sequence (studied for propylammonium substitutions) was intrinsically curved by $\sim 9^\circ$ toward the minor groove. When supplemented with six tethered cations, bending toward the minor groove was enhanced to $\sim 17^\circ$, suggesting that the appended positive charges induced $\sim 8^\circ$ of bending. Acetylation of the tethered amines resulted in a DNA shape indistinguishable from the unmodified duplex, supporting the view that the ammonium cations, rather than the tethers, were responsible for DNA bending.

The $\sim 8^\circ$ of bending induced by cations tethered via propyl groups was smaller than the $\sim 20^\circ$ bend induced when a similar pattern of phosphates was completely neutralized by methylphosphonate substitution (87). However, this result was greater than the $\sim 4^\circ$ bend induced in a different DNA sequence by ammonium ions on longer hexyl tethers (89). These results are summarized in Figure 4. Unlike methylphosphonate analogs, flexible tethers presumably allow some dispersion of appended cations over the DNA surface (52). Dispersion of tethered cations in these model duplexes may be greater than for cationic amino acid side chains in DNA-protein complexes, in which specific cation-phosphate interactions can be stabilized by networks of other contacts. These authors therefore speculated that the bending hierarchy methylphosphonate > propylamine > hexylamine reflected the decreasing extent of phosphate neutralization in this series. It will be interesting to explore DNA bending by cations on more rigid tethers (e.g. 3-aminopropyne) to explore these issues.

Experiments to Manipulate Electrostatic Effects in DNA Bending by Proteins

Strauss-Soukup & Maher also applied the phantom protein model to DNA sequences known to be bent by the binding of specific proteins (92). The PU.1 transcription factor is a member of the Ets family of DNA-binding proteins. PU.1 binds to DNA via a loop-helix-loop domain and functions in the differentiation of hematopoietic cells. The crystal structure of a PU.1-DNA complex has been reported (43). The DNA in this complex is bent by 8° as it engages the protein. The pattern of electrostatic contacts between PU.1 and its DNA-binding site suggested to Kodandapani and coworkers that laterally asymmetric phosphate neutralization accompanies PU.1 binding. Because of the previous studies showing that

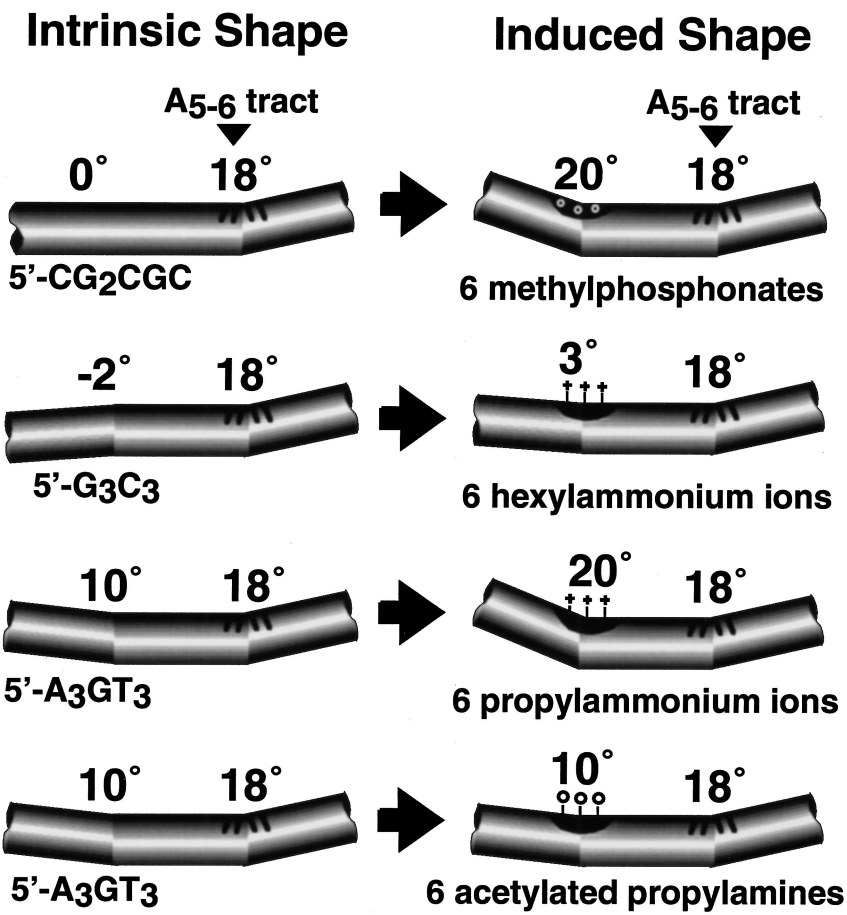

Figure 4 Summary of DNA bending observed by phantom proteins simulated by methylphosphonate substitution (87) or appending cations on propyl (88) or hexyl (89) tethers. Intrinsic DNA shapes of the indicated sequences are shown as cylinders at left, with the position of the reference $A_{5–6}$-tracts noted. Induced shapes are shown at right.

such neutralization can induce bending in naked DNA, the effect of phosphate neutralization by substituting neutral methylphosphonate internucleoside linkages at relevant positions within DNA containing the PU.1-binding sequence was explored. Duplex DNA oligonucleotides composing the PU.1 recognition sequence were synthesized with appropriate phosphates chemically neutralized. Consistent with the prediction that DNA will collapse toward its partially neutralized surface, DNA neutralized at these seven positions to simulate PU.1 binding was observed to bend by 28° (92). The directions of DNA curvature were slightly different in the cocrystal vs the partially neutralized duplexes. The electrostatic component of

the binding energy therefore appeared more than enough to account for the DNA bending observed in the PU.1-DNA complex.

The cases of dimeric basic-zipper (bZIP) DNA-binding proteins, including Fos/Jun (20), Jun/Jun, CREB (65), and GCN4 (17), are also particularly intriguing. Electrophoretic phasing experiments suggest that different members of this family affect DNA shape differently (36–39). The intrinsic shapes of the binding sites for these proteins in DNA have also been shown to differ (45, 65). Amino acids adjacent to the basic region of each bZIP monomer lie near the DNA double helix. It was noted that the pattern of charged amino acid residues in this region correlates with apparent DNA bending in the resulting complex (39, 65). This relationship has been subsequently demonstrated by showing that changing the charges of these residues induces apparent changes in the bend angle of bound DNA (50, 64, 90, 93).

For example, the yeast bZIP transcription factor GCN4 does not induce DNA bending in vitro. Strauss-Soukup and Maher substituted basic residues for three neutral amino acids in GCN4 to produce a GCN4 derivative that appears in electrophoretic phasing assays to bend DNA by $\sim 16^\circ$ (90). This result is consistent with a model of induced DNA bending wherein excess positive charge in proximity to one face of the double helix neutralizes local phosphate diester anions resulting in a laterally asymmetric charge distribution along the DNA, causing collapse of the DNA toward the neutralized surface. When a wider range of charge substitutions was made, the direction and extent of apparent DNA bending by these derivatives were a roughly linear function of the charges of the amino acids adjacent to the basic domain of the protein (93). This relation held over the dimer charge range $+6$ (15.5° apparent bend toward the minor groove) to -6 (25.2° apparent bend toward the major groove). Independent data for mutants of Jun+Fos show similar, roughly linear relationships between peptide charge and DNA bending (50). These data suggest a model in which the trajectory of DNA responds to lateral asymmetries in charge density.

The observation that cationic amino acids positioned on one DNA face induce apparent DNA collapse toward that face suggests that such bZIP proteins can act as class-2 DNA-bending molecules. However, the underlying electrostatic mechanism of DNA bending is not revealed in such experiments. These data have been interpreted in terms of both direct Coulombic attraction (50) and asymmetric phosphate neutralization (64, 90). To directly test the hypothesis that asymmetric phosphate neutralization is responsible for DNA bending by cationic domains of these bZIP proteins, Tomky and coworkers applied the "phantom protein" strategy to measure the effect of partial phosphate neutralization on the shape of the AP-1 bZIP binding site in duplex DNA (97). DNA bending toward the neutralized face of DNA was again observed. The degree of DNA bending induced by methylphosphonate substitution ($\sim 3.5^\circ$ per neutralized phosphate) was comparable with that induced by GCN4 variants carrying increasing numbers of additional basic amino acids. It is therefore plausible that asymmetric phosphate neutralization is the cause of DNA bending in such complexes. Confirmation of these results will

require independent assays of DNA bending by other techniques owing to controversy about interpretation of electrophoretic-phasing experiments with bZIP proteins (50, 54, 84, 85).

FUTURE DIRECTIONS

Phantom Protein Models of Protein/DNA Complexes

It is important to determine the extent to which purely electrostatic effects can explain important biological examples of DNA bending by proteins. Two particularly well-studied cases involve the *E. coli* CAP protein (66, 79) and the nucleosome (53). High-resolution crystal structures now exist for both protein-DNA complexes. In both complexes DNA is highly bent toward the protein-DNA interface (90° over 18 bp in the nucleosome; 90° over 36 bp in the CAP complex). Based on the crystal structures, it is possible to identify cationic amino acid side chains that closely approach the DNA. In the future it may be possible to test the hypothesis that chemical neutralization of the corresponding phosphates will endow the corresponding naked DNA with an intrinsically curved geometry that mimics the shape of DNA in the complex. Quantitative comparison of DNA bending by the "phantom" protein vs bending in the crystal structures will help to estimate the extent to which asymmetric phosphate neutralization contributes to DNA bending in these cases. As described above, initial computer simulations have already addressed these questions for CAP (22).

All-Atom Simulations

An exciting opportunity in molecular mechanics and dynamics modeling is provided by the challenge of exploring DNA bending induced by asymmetries in local charge, whether caused by counterion distributions, bound ligands, bound proteins, or chemical modifications with charged adducts. As described above, important initial contributions have been made with all-atom models of DNA in which solvent and counterions are implicit (22, 47, 78). The development of more complete force fields for DNA and all-atom simulations with explicit solvent and ions has been impressive (34, 103). The availability of such tools leads to optimism that the basis for sequence-specific features of DNA structure may soon be understood at the level of steric and electrostatic factors and that the roles of solvent and ion distributions about the double helix may be elucidated with greater confidence (101, 102).

Effects of Asymmetrically Appended Ions

To date, phantom protein designs have involved chemically neutralizing phosphate diesters or appending monovalent cations asymmetrically about DNA to simulate the binding of class-2 proteins. The intriguing proposal that class-1 DNA-bending

proteins (e.g. TBP) bend DNA away from the binding interface by asymmetrical enhancement of interphosphate repulsions extends the possible role of electrostatic effects (16). The apparent response of DNA shape to GCN4 variants substituted with multiple anionic residues supports the plausibility of this model (93). It is important to devise and study synthetic double helices wherein enhanced interphosphate repulsions are simulated by asymmetrically tethering additional anions.

Oligovalent cations such as Mg^{2+}, $Co(NH_3)_6^{3+}$, and spermidine^{3+} can dramatically alter the physical properties of double-helical DNA (2, 4, 5). A theory to explain reduced DNA longitudinal persistence lengths and, ultimately, DNA condensation has been presented (76). This model suggests that multivalent cations dispersed in the DNA grooves act to cause local DNA collapse, ultimately leading to DNA condensation. This process may be critical for DNA condensation during packaging and other phenomena in vivo. It has been impossible to directly measure bending caused by an isolated multivalent cation such as Co^{3+} bound to a single DNA. Perhaps synthetic strategies for tethering trivalent cations to DNA will allow analysis of their effects on local DNA bending.

DNA Rigidity In Vivo

Although simplified model systems provide tractable tools for measuring electrostatic effects on DNA stiffness, curvature, and bending, these issues are most significant in a cellular context. How important are intrinsic DNA longitudinal and torsional stiffness in the presence of the cellular machinery that handles, folds, unwinds, and reads DNA sequence information during gene expression?

Transcriptional regulation provides an important system for studying the importance of DNA curvature and bending because transcription activator proteins bound at a distance from promoters are thought to function through DNA looping to directly contact their targets (15, 28, 44, 63, 74). DNA looping plays a significant role in the regulation of certain prokaryotic genes including *gal, lac*, and *deo* in *E. coli* (3, 49, 58). Eukaryotic transcription activation is usually depicted such that the DNA intervening between the transcription start site and the sites of activator binding is bent to allow the activators to interact directly with the basal transcription apparatus (69).

Control of eukaryotic transcription initiation therefore involves regulating the affinity of a promoter for the transcription initiation machinery. Transcription activator proteins bound to DNA various distances from the TATA box contribute to promoter affinity. Because most eukaryotic transcription is thought to depend on favorable contributions of DNA-bound activator proteins, the local shape of the tethering DNA should constrain the spatial distribution of these proteins if they are to productively recruit RNA polymerase. Thus, DNA template bending (intrinsic or induced) is predicted to play a critical role in driving protein-protein interactions over the relatively short DNA separation distances commonly encountered for upstream activator-binding sites in promoters (74). The attractive

hypothesis that the inherent physical properties of DNA constrain transcription activation from eukaryotic promoters has been examined in a few studies (18, 41, 77, 95) but should be subjected to systematic experimental verification.

CONCLUSION

Double-helical DNA is a locally stiff polymer in terms of longitudinal-persistence length, torsional rigidity, and resistance to stretching. The physical basis for DNA stiffness remains unresolved. A theoretical model predicts that unbalanced compressive and stretching forces will arise within the double helix upon asymmetric phosphate neutralization (57). We argue that lateral asymmetries in the distributions of counterions and protein cationic side chains both contribute to DNA deformation, based on these electrostatic principles.

ACKNOWLEDGMENTS

LJM expresses appreciation to present and past lab members, particularly A Rodrigues, J Strauss-Soukup, E Ross, P Hardwidge, L Cassiday, and R Den, and acknowledges funding support from NIH grant GM54411 and from the Mayo Foundation. LDW notes the contributions of L McFail-Isom, X Shui, C Sines, and D VanDerveer, and support from NSF grant MCB-9056300 and American Cancer Society grant RPG-95-116-03-GMC. Helpful discussions were provided by V Bloomfield, J Chaires, G Clark, D Crothers, J Feigon, B Gold, P Hagerman, N Hud, J Kahn, G Manning, Y-P Pang, T Record, I Rouzina, J Subirana, and C Switzer.

Visit the Annual Reviews home page at www.AnnualReviews.org

LITERATURE CITED

1. Bartenev VN, Golovamov EI, Kapitonova KA, Mokulskii MA, Volkova LI, Skuratovskii IY. 1983. Structure of the B DNA cationic shell as revealed by an X-ray diffraction study of CsDNA. Sequence-specific cationic stabilization of B form DNA. *J. Mol. Biol.* 169:217–34
2. Baumann C, Smith S, Bloomfield V, Bustamante C. 1997. Ionic effects on the elasticity of single DNA molecules. *Proc. Natl. Acad. Sci. USA* 94:6185–90
3. Bellomy G, Mossing M, Record M. 1988. Physical properties of DNA *in vivo* as probed by the length dependence of the *lac* operator looping process. *Biochemistry* 27:3900–6
4. Bloomfield VA. 1996. DNA condensation. *Curr. Opin. Struct. Biol.* 6:334–41
5. Bloomfield VA. 1998. DNA condensation by multivalent cations. *Biopolymers* 44: 269–82
6. Brukner I, Susic S, Dlakic M, Savic A, Pongor S. 1994. Physiological concentration of magnesium ions induces a strong macroscopic curvature in GGGCCC-containing DNA. *J. Mol. Biol.* 236:26–32
7. Calladine CR. 1982. Mechanics of sequence-dependent stacking of bases in B-DNA. *J. Mol. Biol.* 161:343–52

8. Cantor CR, Schimmel PR. 1980. *Biophysical Chemistry. Part III: The Behavior of Biological Macromolecules*, pp. 979–1039, New York: WH Freeman
9. Crothers D. 1993. Architectural elements in nucleoprotein complexes. *Curr. Biol.* 3: 675–76
10. Crothers DM, Drak J. 1992. Global features of DNA structure by comparative gel electrophoresis. *Meth. Enzymol.* 212:46–71
11. Dickerson RE. 1998. DNA bending: the prevalence of kinkiness and the virtues of normality. *Nucleic Acids Res.* 26:1906–26
12. Dickerson RE, Chiu TK. 1997. Helix bending as a factor in protein/DNA recognition. *Biopolymers* 44:361–403
13. Diekmann S, Wang JC. 1985. On the sequence determinants and flexibility of the kinetoplast DNA fragment with abnormal gel electrophoretic mobilities. *J. Mol. Biol.* 186:1–11
14. Dlakic M, Harrington RE. 1995. Bending and torsional flexibility of G/C-rich sequences as determined by cyclization assays. *J. Biol. Chem.* 270:29945–52
15. Dunaway M, Droge P. 1989. Transactivation of the *Xenopus* rRNA gene promoter by its enhancer. *Nature* 341:657–59
16. Elcock AH, McCammon JA. 1996. The low dielectric interior of proteins is sufficient to cause major structural changes in DNA on association. *J. Am. Chem. Soc.* 118:3787–88
17. Ellenberger TE, Brandl CJ, Struhl K, Harrison SC. 1992. The GCN4 basic region leucine zipper binds DNA as a dimer of uninterrupted alpha helices: Crystal structure of the protein-DNA complex. *Cell* 71: 1223–37
18. Falvo JV, Thanos D, Maniatis T. 1995. Reversal of intrinsic DNA bends in the IFN beta gene enhancer by transcription factors and the architectural protein HMG1(Y). *Cell* 83:1101–11
19. Giese K, Kingsley C, Kirshner JR, Grosschedl R. 1995. Assembly and function of a TCRalpha enhancer complex is dependent on LEF-1-induced DNA bending and multiple protein-protein interactions. *Genes Dev.* 9:995–1008
20. Glover JNM, Harrison SC. 1995. Crystal structure of the heterodimeric bZIP transcription factor c-fos-c-jun bound to DNA. *Nature* 373:257–61
21. Goodman SD, Nash HA. 1989. Functional replacement of a protein-induced bend in a DNA recombination site. *Nature* 341:251–54
22. Gurlie R, Duong TH, Zakrzewska K. 1999. The role of DNA-protein salt bridges in molecular recognition: a model study. *Biopolymers* 49:313–27
23. Hagerman KR, Hagerman PJ. 1996. Helix rigidity of DNA: the meroduplex as an experimental paradigm. *J. Mol. Biol.* 260:207–23
24. Hagerman PJ. 1988. Flexibility of DNA. *Annu. Rev. Biophys. Biophys. Chem.* 17: 265–86
25. Hagerman PJ, 1992. Straightening out the bends in curved DNA. *Biochim. Biophys. Acta* 1131:125–32
26. Harrington RE. 1978. The optico-hydrodynamic properties of high molecular weight DNA. III. The effects of NaCl concentration. *Biopolymers* 17:919–36
27. Honig B, Nicholls A. 1995. Classical electrostatics in biology and chemistry. *Science* 268:1144–49
28. Hori R, Carey M. 1994. The role of activators in assembly of RNA polymerase II transcription complexes. *Curr. Opin. Genet. Dev.* 4:236–44
29. Hud NV, Feigon J. 1997. Localization of divalent metal ions in the minor groove of DNA A-tracts. *J. Am. Chem. Soc.* 119: 5756–57
30. Hud NV, Schultze P, Feigon J. 1998. Ammonium ion as an NMR probe for monovalent cation coordination sites of DNA quadruplexes. *J. Am. Chem. Soc.* 120: 6403–4

31. Hud NV, Sklenar V, Feigon J. 1999. Localization of ammonium ions in the minor groove of DNA duplexes in solution and the origin of DNA A-tract bending. *J. Mol. Biol.* 286:651–60
32. Jack A, Ladner JE, Klug A. 1976. Crystallographic refinement of yeast phenylalanine transfer RNA at 2.5 Å resolution. *J. Mol. Biol.* 108:619–49
33. Jack A, Ladner JE, Rhodes D, Brown RS, Klug A. 1977. A crystallographic study of metal-binding to yeast phenylalanine transfer RNA. *J. Mol. Biol.* 111:315–28
34. Jayaram B, Beveridge DL. 1996. Modeling DNA in aqueous solutions. *Annu. Rev. Biophys. Biomol. Struct.* 25:367–94
35. Kahn JD, Crothers DM. 1993. DNA bending in transcription initiation, *Cold Spring Harbor Symposia Symp. on Quantitative Quant. Biology,* LVIII, 58:115–22. Cold Spring Harbor, NY; Cold Spring Harbor Lab. Press
36. Kerppola TK. 1994. DNA bending specificity among bZIP family proteins. In *Transcription: Mechanisms and Regulation*, ed. R.C. Conaway and, J.W. Conaway, pp. 387–424. New York: Raven
37. Kerppola TK, Curran T. 1991. DNA bending by Fos and Jun: The flexible hinge model. *Science* 254:1210–14
38. Kerppola TK, Curran T. 1991. Fos-Jun heterodimers and Jun homodimers bend DNA in opposite orientations: implications for transcription factor cooperativity. *Cell* 66:317–26
39. Kerppola TK, Curran T. 1993. Selective DNA bending by a variety of bZIP proteins. *Mol. Cell. Biol.* 13:5479–89
40. Kim JL, Nikilov DB, Burley SK. 1993. Co-crystal structure of TBP recognizing the groove of a TATA element. *Nature* 365: 520–27
41. Kim TK, Maniatis T. 1997. The mechanism of transcriptional synergy of an in vitro assembled interferon-beta enhanceosome. *Mol. Cell* 1:119–29
42. Kim Y, Geiger JH, Hahn S, Sigler PB. 1993. Crystal structure of a yeast TBP/TATA-box complex. *Nature*, 365:512–20
43. Kodandapani R, Pio F, Ni C-Z, Piccialli G, Klemsz M, et al. 1996. A new pattern for helix-turn-helix recognition revealed by the PU.1 ets-domain-DNA complex. *Nature* 380:456–60
44. Koleske AJ, Young RA. 1995. The RNA polymerase II holoenzyme and its implications for gene regulation. *Trends Biochem. Sci.* 20:113–16
45. Konig P, Richmond TJ. 1993. The X-ray structure of the GCN4-bZIP bound to ATF/CREB site DNA shows the complex depends on DNA flexibility. *J. Mol. Biol.* 233:139–54
46. Kopka ML, Fratini AV, Drew HR, Dickerson RE. 1983. Ordered water structure around a B-DNA dodecamer. A quantitative study. *J. Mol. Biol.* 163:129–46
47. Kosikov K. 1998. *All-atom computer simulations of "activated" duplex DNA*. PhD thesis. Rutgers Univ., New Brunswick, NJ
48. Laundon CH, Griffith JD. 1987. Cationic metals promote sequence-directed DNA bending. *Biochemistry* 26:3759–62
49. Lee DH, Schleif RF. 1989. *In vivo* DNA loops in *araCBAD*: size limits and helical repeat. *Proc. Natl. Acad. Sci. USA* 86:476–80
50. Leonard DA, Rajaram N, Kerppola TK. 1997. Structural basis of DNA bending and oriented heterodimer binding by the basic leucine zipper domains of Fos and Jun. *Proc. Natl. Acad. Sci. USA* 94:4913–18
51. Li T, Stark MR, Johnson AD, Wolberger C. 1995. Crystal structure of the MATa1/MATa2 homeodomain heterodimer bound to DNA. *Science* 270:262–69
52. Liang G, Encell L, Nelson MG, Switzer C, Shuker DEG, Gold B. 1995. The role of electrostatics in the sequence selective reaction of charged alkylating agents with DNA. *J. Am. Chem. Soc.* 117:10135–36
53. Luger K, Mader AW, Richmond RK, Sargent DF, Richmond TJ. 1997. Crystal structure of the nucleosome core particle at

2.8 Å resolution. *Nature* 389:251–60
54. Maher LJ. 1998. Mechanisms of DNA bending. *Curr. Opin. Chem. Biol.* 2:688–94
55. Manning GS. 1978. The molecular theory of polyelectrolyte solutions with applications to the electrostatic properties of polynucleotides. *Q. Rev. Biophys.* 2:179–246
56. Manning GS. 1988. Three persistence lengths for a stiff polymer with an application to DNA B-Z junctions. *Biopolymers* 27:1529–42
57. Manning GS, Ebralidse KK, Mirzabekov AD, Rich A. 1989. An estimate of the extent of folding of nucleosomal DNA by laterally asymmetric neutralization of phosphate groups. *J. Biomol. Struct. Dyn.* 6: 877–89
58. Matthews KS. 1992. DNA looping. *Microbiol. Rev.* 56:123–36
59. Mirzabekov AD, Rich A. 1979. Asymmetric lateral distribution of unshielded phosphate groups in nucleosomal DNA and its role in DNA bending. *Proc. Natl. Acad. Sci. USA* 76:1118–21
60. Misra VK, Hecht JL, Sharp KA, Friedman RA, Honig B. 1994. Salt effects on protein-DNA interactions. *J. Mol. Biol.* 238:264–80
61. Misra VK, Hecht JL, Yang AS, Honig B. 1998. Electrostatic contributions to the binding free energy of the lambda c1 repressor to DNA. *Biophys. J.* 75:2262–73
62. Muller BC, Raphael AL, Barton JK. 1987. Evidence for altered DNA conformations in the simian virus 40 genome: site-specific DNA cleavage by the chiral complex lambda-tris(4,7-diphenyl-1,10- phenanthrolene)cobalt(III). *Proc. Natl. Acad. Sci. USA* 84:1764–68
63. Muller H-P, Sogo JM, Schaffner W. 1989. An enhancer stimulates transcription in trans when attached to the promoter via a protein bridge. *Cell* 58:767–77
64. Paolella DN, Liu Y, Schepartz A. 1997. Electrostatic mechanism for DNA bending by bZIP proteins. *Biochemistry* 36:10033–38
65. Paolella DN, Palmer CR, Schepartz A. 1994. DNA targets for certain bZIP proteins distinguished by an intrinsic bend. *Science* 264:1130–33
66. Parkinson G, Wilson C, Gunasekera A, Ebright YW, Ebright RE, Berman HM. 1996. Structure of the CAP-DNA complex at 2.5 Å resolution: a complete picture of the protein-DNA interface. *J. Mol. Biol.* 260:395–408
67. Pellegrini L, Tan S, Richmond TJ. 1995. Structure of serum response factor core bound to DNA. *Nature* 376:490–98
68. Pontiggia A, Rimini R, Harley VR, Good fellow PN, Lovell-Badge R, Bianchi ME. 1994. Sex-reversing mutations affect the architecture of SRY-DNA complexes. *EMBO J.* 13:6115–24
69. Ptashne M, Gann A. 1997. Transcriptional activation by recruitment. *Nature* 386:569–77
70. Record MT, Anderson CF, Lohman T. 1978. Thermodynamic analysis of ion effects on the binding and conformational equilibria of proteins and nucleic acids: the role of ion association and release, screening and ion effects on water activity. *Q. Rev. Biophys.* 11:103–78
71. Record MT, Zhang WT, Anderson CF. 1998. Analysis of effects of salts and uncharged solutes on protein and nucleic acid equilibria and processes: a practical guide to recognizing and interpreting polyelectrolyte effects, Hofmeister effects, and osmotic effects of salts. *Adv. Protein Chem.* 51:281–353
72. Rice PA, Yang SW, Mizuuchi K, Nash HA. 1996. Crystal structure of an IHF-DNA complex: A protein-induced DNA U-Turn. *Cell* 87:1295–1306
73. Rich A. 1978. Localized positive charges can bend double helical nucleic acids. *FEBS Lett.* 51:71–81
74. Rippe K, von Hippel PH, Langowski J. 1995. Action at a distance: DNA-looping

and initiation of transcription. *Trends Biol. Sci.* 20:500–6
75. Rosenberg JM, Seeman NC, Kim JJP, Suddath FL, Nicholas HB, Rich A. 1973. Double helix at atomic resolution. *Nature* 243:150–54
76. Rouzina I, Bloomfield A. 1998. DNA bending by small, mobile multivalent cations. *Biophys. J.* 74:3152–64
77. Ruden DM, Ma J, Ptashne M. 1988. No strict alignment is required between a transcriptional activator binding site and the "TATA box" of a yeast gene. *Proc. Natl. Acad. Sci. USA* 85:4262–66
78. Sanghani S, Zakrzewska K, Lavery R. 1996. Modeling DNA bending induced by phosphate neutralisation. In *Biological Structure and Dynamics*, ed. R Sarma, M Sarma, pp. 267–78. Schenectady, NY: Adenine
79. Schultz SC, Shields GC, Steitz TA. 1991. Crystal structure of a CAP-DNA complex: The DNA is bent by 90°. *Science* 253: 1001–7
80. Shlyakhtenko LS, Lybubchenko YL, Chernov BK, Zhurkin VB. 1990. Influence of temperature and ionic strength on electrophoretic mobility of synthetic DNA fragments. *Mol. Biol. (Moscow)* 24:79– 95
81. Shore D, Langowski J, Baldwin RL. 1981. DNA flexibility studied by covalent closure of short fragments into circles. *Proc. Natl. Acad. Sci. USA* 78:4833–37
82. Shui X, McFail-Isom L, Hu GG, Williams LD. 1998. The B-DNA dodecamer at high resolution reveals a spine of water on sodium. *Biochemistry* 37:8341–55
83. Shui X, Sines C, McFail-Isom L, VanDerveer D, Williams LD. 1998. Structure of the potassium form of CGCGAATTCGCG: DNA deformation by electrostatic collapse around inorganic cations. *Biochemistry* 37:16877–87
84. Sitlani A, Crothers DM. 1998. DNA-binding domains of Fos and Jun do not induce DNA curvature: an investigation with solution and gel methods. *Proc. Natl. Acad. Sci. USA* 95:1404–9
85. Sitlani A, Crothers DM. 1996. Fos and jun do not bend the AP-1 recognition site. *Proc. Natl. Acad. Sci. USA* 93:3248–52
86. Stigter D. 1998. An electrostatic model for the dielectric effects, the adsorption of multivalent ions, and the bending of B-DNA. *Biopolymers* 46:503–16
87. Strauss JK, Maher LJ. 1994. DNA bending by asymmetric phosphate neutralization. *Science* 266:1829–34
88. Strauss JK, Prakash TP, Roberts C, Switzer C, Maher LJ. 1996. DNA bending by a phantom protein. *Chem. Biol.* 3:671–78
89. Strauss JK, Roberts C, Nelson MG, Switzer C, Maher LJ. 1996. DNA bending by hexamethylene-tethered ammonium ions. *Proc. Natl. Acad. Sci. USA* 93:9515–20
90. Strauss-Soukup JK, Maher LJ. 1997. DNA bending by GCN4 mutants bearing cationic residues. *Biochemistry* 36:10026–32
91. Strauss-Soukup JK, Maher LJ. 1997. Effects of neutralization pattern and stereochemistry on DNA bending by methylphosphonate substitutions. *Biochemistry* 36:8692–98
92. Strauss-Soukup JK, Maher LJ. 1998. Electrostatic effects in DNA bending by GCN4 mutants. *Biochemistry* 37:1060–66
93. Strauss-Soukup JK, Maher LJ. 1997. Role of asymmetric phosphate neutralization in DNA bending by PU.1. *J. Biol. Chem.* 272: 31570–75
94. Swarnalatha Y, Yathindra N. 1993. Stereochemical effects of methylphosphonate in B- and Z-DNA helices: variation in hydrophobicity and effective widths of grooves. *J. Biomol. Struct. Dyn.* 10:1023–45
95. Takahashi K, Vigneron M, Matthes H, Wildeman A, Zenke M, Chambon P. 1986. Requirement of stereospecific alignments for initiation from the simian virus 40 early promoter. *Nature* 319:121–26
96. Tereshko V, Minasov G, Egli M. 1999. A "hydrat-ion" spine in a B-DNA minor groove. *J. Am. Chem. Soc.* 121:3590–95

97. Tomky LA, Strauss-Soukup JK, Maher LJ. 1998. Effects of phosphate neutralization on the shape of the AP-1 transcription factor binding site in duplex DNA. *Nucleic Acids Res.* 26:2298–2305
98. Werner MH, Burley SK. 1997. Architectural transcription factors: Proteins that remodel DNA. *Cell* 88:733–36
99. Werner MH, Gronenborn AM, Clore GM. 1996. Intercalation, DNA kinking, and the control of transcription. *Science* 271:778–84
100. Wing R, Drew H, Takano T, Broka C, Takana S, et al. 1980. Crystal structure analysis of a complete turn of B-DNA. *Nature* 287:755–58
101. Young MA, Beveridge DL. 1998. Molecular dynamics simulations of an oligonucleotide duplex with adenine tracts phased by a full helix turn. *J. Mol. Biol.* 281:675–87
102. Young MA, Jayaram B, Beveridge DL. 1997. Intrusion of counterions into the spine of hydration in the minor groove of B-DNA: fractional occupancy of electronegative pockets. *J. Am. Chem. Soc.* 119: 59–69
103. Young MA, Ravishanker G, Beveridge DL. 1997. A 5-nanosecond molecular dynamics trajectory for B-DNA: analysis of structure, motions, and solvation. *Biophys. J.* 73:2313–36